

Advanced Photonic Circuit Simulation

Steven R.A. Dods, Jackson Klein, and Z. Jan Jakubczyk
Optiwave Systems, 7 Capella Ct., Ottawa, K2E 8A7, Canada

ABSTRACT

Planar Photonic Circuits can perform many useful functions in optical communications systems, such as wavelength division multiplexing (WDM), optical channel add/drop, fibre/waveguide coupling, and amplifier gain equalization. They perform these functions by the interaction of the device structure with the light inside them. There are very effective and proven numerical methods available for modelling this interaction, such as the Beam Propagation Method (BPM), the Finite Difference Time Domain (FDTD) method, and coupled mode theory (CMT). However, these methods work on a microscopic level (typically the smallest distance is about 0.1 microns), but photonic circuits, on the other hand, can occupy an entire wafer (scale: 10 cm). The analysis must span 5 or more orders of magnitude in the change in scale. The successful analysis needs to combine the basic microscopic techniques with an approach at a more abstract, or system, level. It is interesting that software designed for the analysis of optical communication systems can be applied to planar photonic circuits. This paper shows an example of a practical photonic circuit, a lattice filter, that cannot be analysed by BPM alone. It will be demonstrated that when used with a system level analysis, the whole device can be simulated.

Keywords: Integrated Optics, optical waveguides, photonic circuits, lattice filter, BPM, WDM

1. Introduction

Photonic circuits have much in common with electrical circuits, and so it is not surprising to find electronic techniques being applied to the optical domain. Techniques of digital filter synthesis have been successfully adapted for optical filter synthesis [1], [2]. Using these techniques, it is possible to design filters having specifications as close as physically possible to the desired characteristics. The realization of a digital filter is only limited by what can be achieved in digital electronic circuits. However, photonic circuits have different constraints which are related to the technology of optical waveguides. The limitations imposed by limits on radius of curvature are hard to define in any theory, and are more usually addressed by an empirical or numerical approach. Optical circuits must conform to certain design rules, waveguides usually need to be connected such that the tangents at the endpoints are parallel, and sometimes need to be offset to reduce coupling loss due to changes in curvature [3]. When taken with limitations on the radius of curvature, and limitations on the size of the wafer, even the geometry of the layout can impose constraints that are hard to define in advance. Naturally, none of this is in the scope of the synthesis theory, and so at some point the result of synthesis needs to be assessed by optical waveguide analysis. The analysis of optical waveguides is typically numerically intensive, but usually only a few common techniques are required to address most problems, so commercial software is practical for this part of the task [4].

In this paper we present an example of the design of a lattice filter for isolation of a single optical channel defined by the ITU grid [5]. This example illustrates the typical challenge encountered in design of planar photonic circuits. The large scale range of the analysis (100 nm to 10 cm, 5 orders of magnitude), makes it necessary to combine microscopic analysis methods with those on a system level. The synthesis technique used for the lattice filter was first introduced by Jinguji and Kawachi [1], and is also illustrated in Ref 2. The end product of the analysis in photonic circuit design is a mask for fabrication, the application of a synthesis technique to obtain a design is only the first step. Therefore we illustrate as many of the following steps as possible, showing at each stage how software can be used to aid the process.

2. Photonic Circuit Example: Lattice Filter

As an example of a device that needs a system kind of analysis, this paper presents a lattice filter with specs suitable for ITU grid applications[5]. A schematic of the layout is shown in Fig. 1.

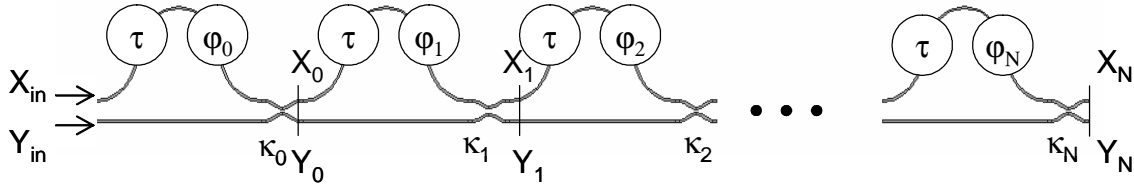


Fig. 1, Schematic of lattice filter. τ is the optical delay, ϕ the phase shift, κ the coupling coefficient.

The device takes light in the fundamental mode of the waveguide, and may enter at either of the waveguides on the left. The lattice filter consists of a planar network of waveguides. There are regions where the waveguides become close enough for some optical coupling, passage of light from one waveguide to the other (optical coupler). The couplers are connected by pairs of waveguides of unequal length. The light will take a longer time to reach the next coupler on the curved path than the straight path. This delay is denoted τ . The delay is the same in all the waveguide pairs, although there may be a very short additional length that can be expressed as a phase shift, ϕ . Of course, this means that the optical delays are in fact unequal, however, as will be shown in Section 2.2, there is a huge conceptual advantage to thinking of these lengths as equal, and accounting for the difference with a phase shift. This phase shift, attained as it is by an additional length of waveguide, will vary with optical frequency, and is not, strictly speaking, a constant phase shift. However, the ITU specification is a narrow band one (ranging from 197.1 to 186.7 THz), so this phase shift will not vary significantly over the whole ITU spectrum. The coupling level (the fraction of light transferred to the other waveguide) is not usually the same in each coupler. The lattice filter design problem is therefore to find the coupling coefficients and phases that will achieve a useful function, such as a selective filter for optical frequencies.

2.1 Lattice Filter Analysis

To discover the possibilities with this device, the first step is to perform an elementary analysis. A schematic of one of the couplers is shown in Fig. 2, with labels at the input and output ports of the coupler, which represent the complex amplitude of the fundamental mode of the waveguide (an optical phasor), with all waves travelling from left to right.

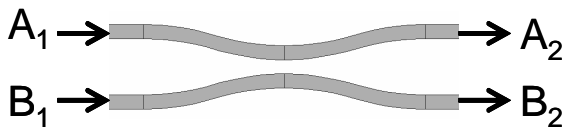


Fig. 2, Two port coupler

The relation between the inputs (A_1 and B_1) and the outputs (A_2 , B_2) comes from a solution to the Maxwell equations, which we solve by the BPM. Since the Maxwell's equations are linear, it is possible to form new solutions from linear combinations of already found solutions, and so all possible solutions can be characterized with a matrix. Two convenient solutions to start with are those corresponding to initial conditions $A_1 = 1$ and $B_1 = 0$, and $A_1 = 0$ and $B_1 = 1$. These solutions, when resolved into the output complex amplitudes A_2 and B_2 , form the columns of the system matrix, S_c .

$$\begin{bmatrix} A_2 \\ B_2 \end{bmatrix} = \begin{bmatrix} S_{c11} & S_{c12} \\ S_{c21} & S_{c22} \end{bmatrix} \begin{bmatrix} A_1 \\ B_1 \end{bmatrix} \quad (1)$$

It is usual for reference planes 1 and 2 to have their own time origins, with the time origin 2 later than 1 by the time of transit from 1 to 2 at the speed of the optical wave. With the time origins defined this way, the matrix S does not depend strongly on wavelength, and can usually be considered constant. In any case it is independent of the initial conditions at 1.

If the coupler is well designed to avoid losses, it can be considered loss-less. In this case, one constraint on the matrix is that $S_c^T \bar{S}_c = I$, and consideration of symmetry of the design requires the matrix be symmetric. As a result, the matrix reduces to a function of one variable, κ , the fraction of power that crosses from one waveguide to the other:

$$\begin{bmatrix} A_2 \\ B_2 \end{bmatrix} = \begin{bmatrix} \sqrt{1-\kappa} & -j\sqrt{\kappa} \\ -j\sqrt{\kappa} & \sqrt{1-\kappa} \end{bmatrix} \begin{bmatrix} A_1 \\ B_1 \end{bmatrix} \quad (2)$$

The output of the coupler can be cascaded with the waveguides that connect it to the next coupler. With the time reference of the reference planes adjusted so that the straight waveguides have no contribution, the effect of the curved waveguide is modelled by an optical delay of time τ in the curved path, the differential delay. When using the digital filter theory, it is usual to normalize frequencies by this delay time. If the actual optical frequency in rad/sec is Ω , then the normalized frequency is written as $\omega = \Omega \tau$. In the frequency domain, we use a positive definition of time, with the actual value of field components recovered from the real part of the complex field multiplied by $\exp[j\Omega t]$, or $\exp[j\omega t / \tau]$. With this normalization and time sense, the relative delay on the curved waveguide is modelled by multiplying the phasor at the input by $e^{-j\omega}$. In matrix form, one step in the lattice can be calculated by forming the matrix product

$$\begin{bmatrix} X_n \\ Y_n \end{bmatrix} = S_n \begin{bmatrix} X_{n-1} \\ Y_{n-1} \end{bmatrix} \quad (3)$$

where

$$S_n = \begin{bmatrix} \sqrt{1-\kappa_n} & -j\sqrt{\kappa_n} \\ -j\sqrt{\kappa_n} & \sqrt{1-\kappa_n} \end{bmatrix} \begin{bmatrix} e^{-j\phi_n} e^{-j\omega} & 0 \\ 0 & 1 \end{bmatrix} \quad (4)$$

Since one step in the lattice can be calculated this way, the matrix for the whole lattice can be found by multiplying the steps

$$S = S_N S_{N-1} \cdots S_1 S_0 \quad (5)$$

2.2 Lattice Filter Synthesis

Lattice filter synthesis starts by employing the Z-Transform

$$z = e^{j\omega} \quad (6)$$

The motivation for moving the analysis to the complex z plane is that, after the multiplications of S_n in (5) are performed, the resulting four elements of S will be polynomials of order N and $N+1$ in z . (The polynomials in the left column come out one order higher than the ones in the right column). Polynomials are more amenable to theoretical analysis than are transcendental functions, so the system matrix is more easily understood in the z plane than in the ω plane. The polynomial can be factored into N complex roots, and the function can be understood in terms of positions of zeros in the complex z plane. In planar circuits that contain rings (where the output of a coupler is connected back to an input), the system matrix is a rational function. It consists of a finite number of poles as well as zeros, and some researchers have found this graphical interpretation useful in its own right [6].

Suppose the matrix multiplication in (5) has been carried out, and the S_{11} matrix element is written out as a polynomial A in z :

$$S_{11}(z) = z^{-1}A_N(z) \quad (7)$$

where

$$A_N(z) = a_0 + a_1z^{-1} + a_2z^{-2} + \dots + a_Nz^{-N} \quad (8)$$

Suppose the lattice is excited at X_{in} in Fig. 1 with a short optical pulse of length much shorter than τ . The light will be divided in two unequal parts by the first coupler, with a fraction κ_0 of the input power going to the lower waveguide path, Y . The light that enters the Y path will be divided again at the next coupler. Since the fraction of the pulse that entered the X path at 0 has not yet arrived at point 1, we can predict that after the second coupler, the power of the first pulse in the Y path will be $\kappa_0(1 - \kappa_1)$. One can trace this path out to X_N , and predict the fraction of power that arrives in the first output pulse. The path being described is the fastest path through the filter, having unit delay in the normalized units, corresponding to a term of z^{-1} in polynomial (7). The coefficient of this term is a_0 in (8). Similarly, we can identify a slowest path, the one that goes through all $N+1$ delays. Therefore the output at X_N will consist of $N+1$ pulses, each with amplitude a_n . By setting a rule that the optical delay should be the same for each stage of the filter, it is possible to use the Z-Transform, in which the output of any such filter is characterized by N th order polynomials in z .

This linear system has the same kind of impulse response as the moving average or Finite Impulse Response (FIR) digital filter. In the digital FIR filter, the input is sampled at rate τ and the digital circuit stores N samples from the recent past. The output is formed as a linear combination of the $N+1$ samples that exist at any instant. The objective of the digital FIR design is the same as the optical lattice filter design: find the best choice of coefficients a_n such that the response $A_N(z)$ approaches a desired function. In the digital filter design, as in the lattice filter design, it is only the value of A_N over the unit circle in the z plane that is important, since the transfer function is obtained by reusing the Z transform, substitution (6).

This optimization problem has been solved in the digital FIR filter design. The technique implemented is known as the Remez exchange algorithm, which is inspired from the Alternation Theorem. Briefly, this is an observation that the best results are obtained when the function A_N has $N+2$ extrema as ω varies from 0 to π . Although initially neither these extremal frequencies or the corresponding a_n are known, it is possible to set up an iterative process whereby the extrema are guessed at, and the resulting a_n found. Once the actual extrema for that choice is found, they are used as the next guess, and so on [7]. The algorithm is well known in the field of digital signal processing, and is available as commercial software. We used Matlab, which has a toolbox for signal processing [8].

At this point, the general form of the result of any lattice filter is represented by (8), and a suitable algorithm is available to select the unknown coefficients in the polynomial. Once those coefficients have been selected, the lattice filter itself (the values of the coupling coefficients at each coupler) can be reconstructed by an iterative process. The reconstruction can be considered the solution of an inverse problem, since the system is being reconstructed from a knowledge of the spectrum. The details of the reconstruction are not presented here, since they are well described elsewhere [1] [2, page 198 to 206].

We present an example applied to the design of a lattice filter for isolation of a single optical channel defined by the ITU grid. The spacing between channels is 100 GHz, and the usual requirement is to isolate the given channel from the nearest and next nearest neighbour. This means the Free Spectral Range (FSR) of the filter should be at least 300 GHz. The FSR is determined by the differential delay τ in the lattice filter stages. We set $\tau = 3.2$ ps to obtain an FSR of 312.5 GHz. In normalized units, the stop bandwidth, 100 GHz, is 0.32. High speed optical links, on the other hand, can require 40 GHz bandwidth, so the pass band should be set, in normalized units, to 0.128. We selected $N = 14$ and ran the Remez exchange algorithm to obtain the coefficients found in Table 1. When the coefficients in the second column of Table 1 are used in (8), and the function is evaluated over the optical frequency by evaluating the function over the unit

circle in the z plane, as suggested from the substitution $z = e^{j\omega}$, a very good approximation to an ideal band pass filter is obtained. However, upon checking the maximum value of the transfer function, it is found to be slightly greater than 1, + 0.236 dB. While this is not a problem in digital filter synthesis, it does pose a problem for optical filter synthesis. The proposed optical filter is a passive device, and so the transfer function must be less than or equal to 1 for all frequencies. The usual choice is to modify the Remez exchange result by reducing all coefficients by a common factor, so as to obtain a maximum transfer function of unity. The coefficients normalized this way are shown in column 3 of Table 1.

n	a_n	normalized a_n	κ_n	ϕ_n
0	-0.02681	-0.02609	0.99868	-
1	-0.02655	-0.02584	0.00349	$-\pi$
2	-0.01534	-0.01492	0.00502	0
3	0.02169	0.02111	0.00165	0
4	0.08197	0.07977	0.00280	π
5	0.15052	0.14649	0.04434	0
6	0.20514	0.19965	0.14503	0
7	0.22600	0.21994	0.20877	0
8	0.20514	0.19965	0.14503	0
9	0.15052	0.14649	0.04434	0
10	0.08197	0.07977	0.00280	0
11	0.02169	0.02111	0.00165	π
12	-0.01534	-0.01492	0.00502	0
13	-0.02655	-0.02584	0.00349	0
14	-0.02681	-0.02609	0.00132	0

Table 1, The coefficients of the lattice filter polynomial and the required coupling coefficients and phase shifts

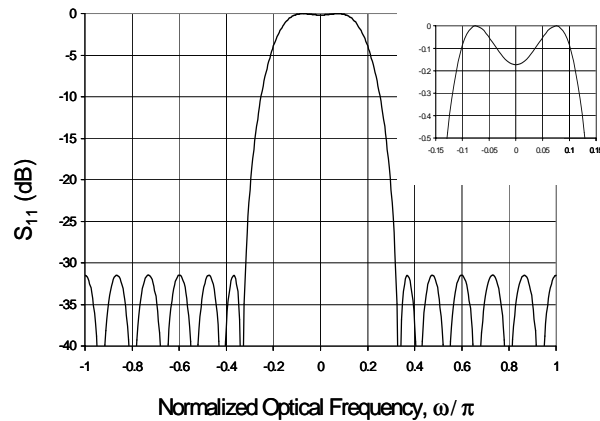


Fig. 3, The expected spectral response of the lattice filter

The expected transfer function is shown in Fig. 3. The passband has a maximum insertion loss of 0.5 dB, and the stopband rejection ratio is greater than 31 dB.

Applying the synthesis of algorithm of Ref 1 gives the coupling coefficients and phase shifts for the lattice filter, shown in columns 4 and 5 of Table 1. To begin the synthesis algorithm, it is necessary to find a suitable polynomial for the other arm of the lattice filter, corresponding to the matrix component S_{21} . This polynomial is not arbitrary, but it is not unique either, it must be selected among a list of possibilities. The possibilities come from the observation that the product of determinants is equal to the determinant of products in the multiplication in (5), and the determinant of the system matrix is known in advance, owing to the unimodular property of the coupler matrix. The other polynomial can be constructed by selecting N roots from the $2N$ roots available. The selection process is known as spectral factorization, and our solution was found by selecting the roots found inside the unit circle. The synthesis algorithm works by taking advantage of the fact that it is easy to gain information about the first and last coefficients in the polynomial A_N , since there is only one path through the filter that has the minimum or maximum delay. For this reason it is easy to determine the coupling coefficient and phase delay of the last coupler. Once the details of the last coupler are found, the system matrix for the lattice with $N-1$ stages is found by multiplying by the single stage system matrix S_{N-1}^{-1} . Once this system matrix for the shortened-by-one-stage filter is found, the process is repeated to find the next stage, until the whole filter is reconstructed.

One feature of the solution obtained from the synthesis algorithm is that all the coupling coefficients are small, with the exception of the first one, which is close to unity (all power crossing over). As will be shown in Section 2.5, a small value of coupling coefficient can be realized more reliably than a large one, so the spec of the first coupler is undesirable. On the other hand, if the input is changed from X_{in} to Y_{in} , and the coupling coefficient set to $1 - \kappa_0$, (and the π phase shift

removed), the same optical transfer function will be obtained. The device with smaller coupling coefficients should be easier to fabricate, being less sensitive to fabrication errors.

2.3 Photonic Circuit, System Level Analysis

Photonic circuits such as the lattice filter can be analysed by employing a suitable system level CAD, such as OptiSystem [9]. The CAD has a layout in which the optical elements, such as couplers, phase shifts, and optical delays can be placed and connected in the appropriate way. Fig. 4 shows

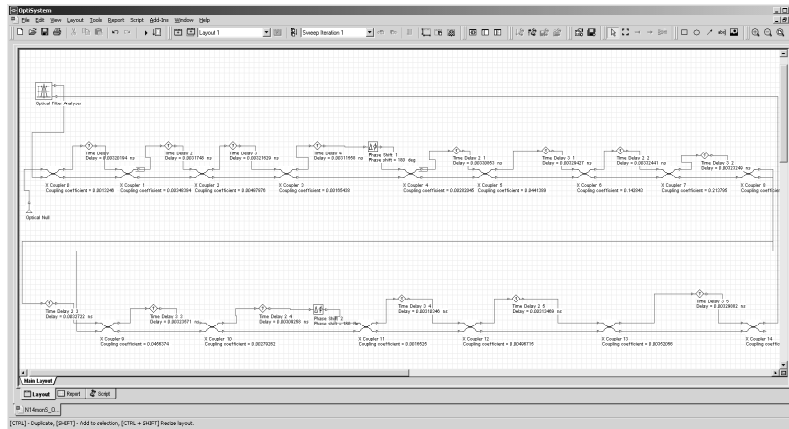


Fig. 4, Schematic for System Level analysis of a photonic circuit

the layout of the circuit of Table 1. The couplers, phase shift, and delay components are dragged and dropped into the layout, the parameters are set through dialog boxes that address each component, and the terminals on the components are connected in any way, provided that inputs are connected only to outputs and vice versa. The component Optical Filter Analyser in the upper left part of the layout sends an optical signal of unit amplitude out, and compares this with the return wave. This analysis is in the wavelength domain, the output is scanned over a range of wavelengths, and the result is, of course, the same as the theoretical design of Fig. 3.

OptiSystem analysis can also be done in the time domain. Since the lattice filter has a simple response to a short pulse, it is useful to replace the source of Optical Filter Analyser in Fig. 4 with a short pulse optical source, and then observe the result in the time domain, as shown in Fig. 5.

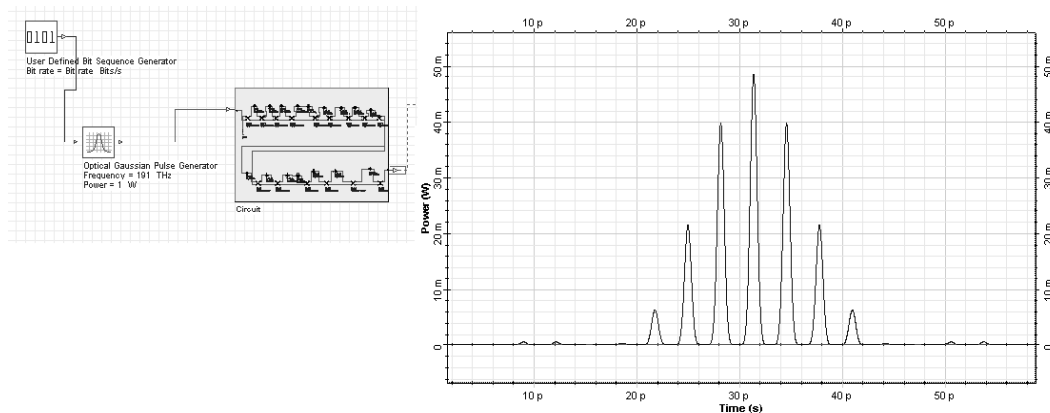


Fig 5, Short pulse input to the circuit, and resulting time response. In this simulation, the bit rate is set to 390 GB/s, so the pulse width of 0.3 bit in the pulse generator creates a sub-picosecond pulse, to clearly resolve the coefficients of the Z transform polynomial.

There are 15 pulses on the output, corresponding to the 15 coefficients in the polynomial (8). The amplitudes of the pulses are equal to the squares of the coefficients in the third column of Table 1. So far, the simulation by software simply confirms the synthesis algorithm result. However, in section 2.6 the parameters will be changed to simulate the effects of errors in fabrication.

2.4 Photonic Circuit, Device Level Analysis

The ultimate aim of the design is a mask to use for fabrication of the device. The above analysis has provided some of the basic specifications for the design, such as the required optical delay and the coupling coefficients for the couplers. However, these specifications must be achieved in an optical circuit that conforms to certain design rules. The waveguides need to be connected such that the tangents at the endpoints are parallel, and the limits on the radius of curvature and possible bend coupling losses need to be investigated. For this task a software specialized to optical device design, such as OptiBPM [9], can be used to advantage.

We choose values typical for waveguides made in silica, with a cladding index of 1.480 and core index of 1.500. The waveguide cross section is a square of $4 \times 4 \mu\text{m}$. At an optical wavelength of $1.55 \mu\text{m}$, OptiBPM predicts this is a single mode waveguide with modal index 1.49007. OptiBPM can predict loss and other effects of bending by direct simulation of a curved waveguide, but the best results are obtained by applying the conformal mapping method [10-12]. This method uses conformal mapping in the complex plane to transform a curved waveguide in the original coordinate system into a straight waveguide with a modified refractive index in a new coordinate system. The transformation is very convenient for the BP method because, in the new coordinate system, the problem is paraxial, and the bend can be maintained for as many revolutions as desired. In practice, the bend is propagated until the power loss is large enough to make an accurate estimate of the bend loss.

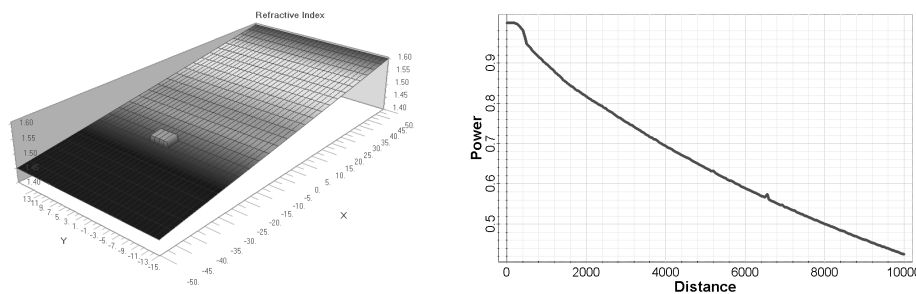


Fig 6, Bend loss estimation by Conformal Mapping method. On the left is the perturbed refractive index corresponding to a bend radius of 1 mm, on the right is the power in the calculation window as a function of propagation distance in microns.

When the waveguide is bent, the mode travels a greater distance with increasing radius. The conformal mapping method works by increasing the refractive index to make the optical distance greater at larger radius. The mode responds by leaking into the region of greater index, simulating the loss of light from a bend. The power curve shows some discontinuity at the position where the bend begins. This is a temporary response due to the coupling from the straight waveguide mode field pattern to the bent waveguide mode field pattern. After this, the power loss settles to an exponential decay, and the loss coefficient can be estimated from the rate of decay. As seen from Fig. 6, a bend radius of 1 mm is too small for this waveguide. At a larger bend radius, 3 mm, the bend loss was found to be negligible (about $1e-6 / \text{cm}$). However, even at this bend radius, there is a small coupling loss, about 0.02 dB. This loss is important because it is experienced every time the waveguide changes its curvature. Secondly, it will be about twice this size at the points of inflection of the S bends used to make the delayed path. Since there are 14 stages in the filter each with 4 changes in curvature, this loss will accumulate to 1.6 dB. Numerical experiments suggest that introducing a waveguide offset of $0.08 \mu\text{m}$ can reduce the coupling loss in dB by an order of magnitude. Third, this loss accumulates only in the curved path, so its effect will be add distortion as well as contributing to the insertion loss. This problem with asymmetry could be overcome by introducing similar losses in the straight path by putting offsets in that path as well, if necessary. In that case the loss would contribute only to insertion loss, and not to degrading the other filter specifications.

The BPM analysis of the bent waveguide will show another important feature, the modification of the modal index by the curve. This can be observed directly by noting the change in phase of the wave as it propagates through the conformal region. The reference index is set to the modal index of the straight waveguide, but a linear decline of phase over 1 cm of -1.722 was observed. This decline can be used to calculate the modal index of the bent waveguide.

Writing n_0 for the straight modal index and n' for the bent one, $\Delta\phi = k(n_0 - n')L$, which implies

$n' = n_0 - \lambda\Delta\phi / 2\pi L$. The result is $n' = 1.49011$, a change in modal index of about 4.2×10^{-5} . It is interesting to

compare this with the thermo-optic effect, since tuning of such devices is often achieved by local heating of different parts of the circuit. In silica a reasonable value for this coefficient is $8.3 \times 10^{-6} / ^\circ\text{C}$, therefore the effect of the bend corresponds to a temperature shift of about 2°C . If temperature based control greater than 2°C is expected, the effect of the waveguide bend on modal index could be neglected in this example.

The next task is to create a suitable layout for the circuit given the constraint of radius of curvature. The essential feature is that the curved path in Fig. 7 needs to give the required time delay of 3.2 ps for the loops without phase shift. This delay is expressed as an optical path length by multiplying by the speed of light, $s_0 = c\tau = 959.336 \mu\text{m}$. The required optical length for the 3.2 ps delay plus a phase shift of π is $960.121 \mu\text{m}$.

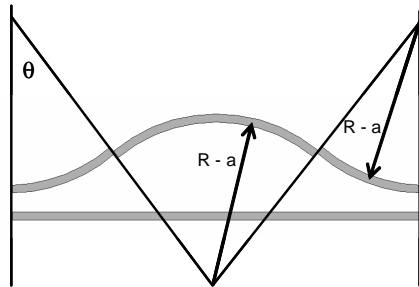


Fig. 7, Geometry for one of the loops of the lattice filter. The radius of curvature of the circular arcs, R is reduced by the waveguide offset, a .

Writing the waveguide offset as a , and the original radius of curvature as R , the geometry of the lattice filter loop comes from solving the following transcendental equation for the angle, θ

$$4Rn \sin \theta + s_0 - 4n'(R - a)\theta = 0 \quad (9)$$

The total length of the device can be shortened by bending the straight waveguide in an arc with radius R in the 8th lattice stage. The resulting layout can be fit in a wafer of length 7 cm. Due to the scale of the layout, it is not possible to see certain details, such as the waveguide offsets at the junction where waveguide curvature changes, and that in each of the couplers the minimum waveguide separation is different, to achieve the required coupling coefficient for each stage.

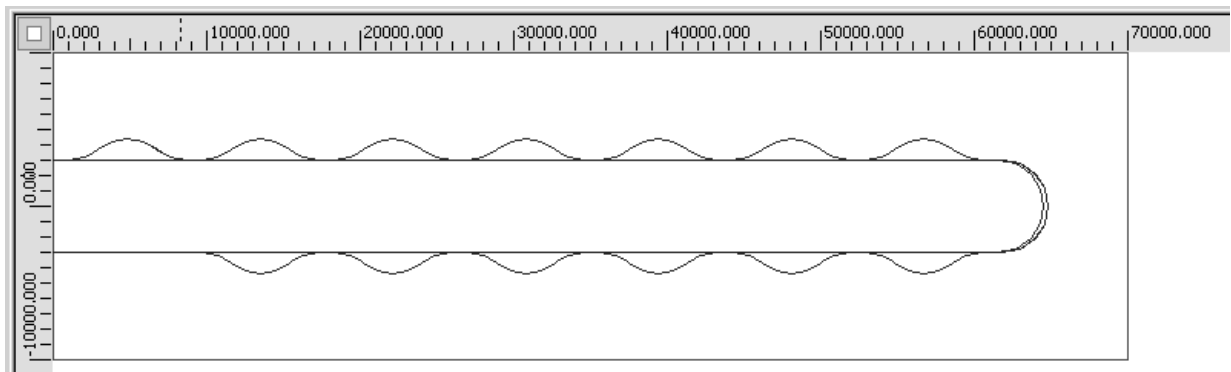


Fig. 8, The lattice filter mask layout. Scale in microns.

2.5 Sensitivity Analysis, Device Level

On the device level, it is possible to investigate the sensitivity of device performance on the inevitable errors in fabrication. Although theoretical models cannot model all possible deviations from the ideal, some deviations, such as those caused by an error in waveguide width, can be estimated. We assume the accuracy of the lithography process to be $\pm 0.1 \mu\text{m}$, and then repeat calculations of modal index and coupling coefficient to estimate the departure from the ideal value. The numerical analysis is used to determine the sensitivity of the parameter to the variation of the process variable. In this example, the rate of change of coupling coefficient with respect to waveguide width, m , is calculated. The RMS value of the coupling coefficient is then m times the RMS value of the width. This variation depends on the coupling coefficient itself, because the higher coefficients are obtained by making the waveguides in the coupler closer together. This proximity makes the coefficient more sensitive to variations in waveguide width. Table 2 shows the design value for each coupling coefficient and the RMS variation expected for each.

n	κ_n	RMS(κ_n)
0, 14	.001324	4.23e-6
1, 13	.003492	1.97e-5
2, 12	.005018	4.32e-5
3, 11	.001653	1.43e-6
4, 10	.002796	9.94e-6
5, 9	.044342	9.48e-4
6, 8	.145027	3.85e-3
7	.208767	6.09e-3

Table 2, RMS variation of coupling coefficients, calculated from variation of waveguide width. The waveguide width deviated from the design value by $\pm 0.1 \mu\text{m}$, with a uniform distribution.

The sensitivity of the modal index to waveguide width variation can be calculated in the same way. In fact, the necessary data, the rate of change of the modal index with waveguide variation, comes as a byproduct of the BPM calculation of table 2. The software automatically calculates and reports the modal index in order to set the reference index for the coupler calculation. From this data it was calculated that the rate of change of modal index with respect to waveguide width is 0.001578. Calling this slope m , and assuming a uniform distribution of waveguide width error, the RMS variation of the modal index should be $m(0.1)/\sqrt{3} = 9.1\text{e-}5$. It is interesting to note that in thermo-optic terms, this variation should correspond to a temperature variation of about 10°C . This variation in modal index is translated into variation of differential delay in the stages of the lattice filter. If L is the physical length difference in one of the lattice filter stages, then the delay is $\tau = nL/c$. The RMS variation of the delay is therefore

$$RMS(\tau) = \frac{L}{c} RMS(n) = \tau \frac{RMS(n)}{n} = 0.19 \text{ fs} \quad (10)$$

2.6 Sensitivity Analysis, System Level

The sensitivity of device level properties to an expected fabrication error has been calculated in the previous section. These results are now fed back to the system level analysis to calculate the expected errors in the end result – the transfer function of the filter.

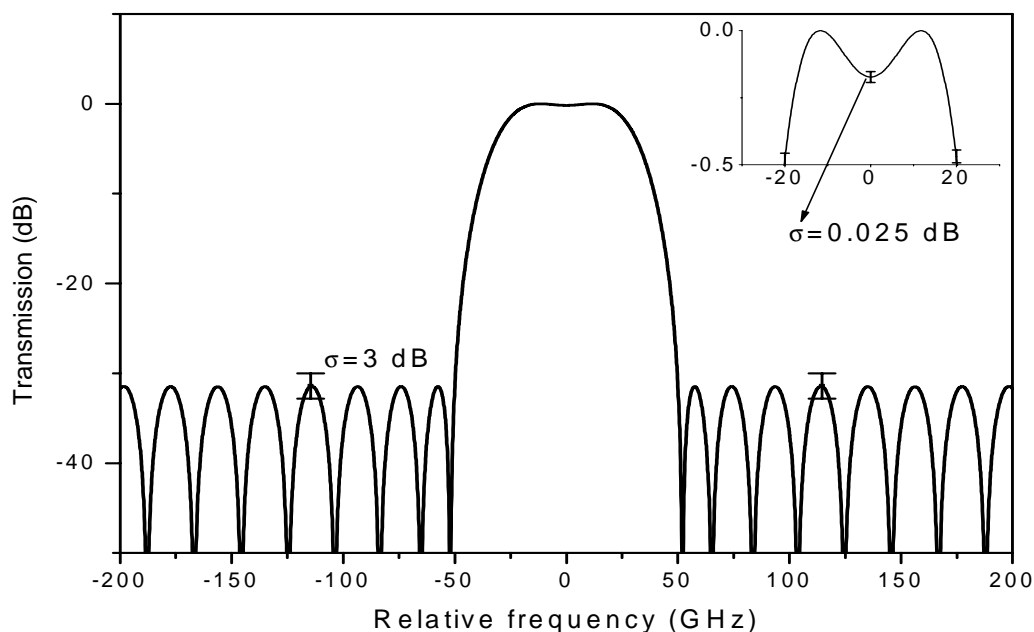


Figure 9, spectral response of the filter, as calculated by OptiSystem, including the error bars at the pass band and stop band.

During the system level analysis, the transfer function of the filter was calculated 5000 times using the parameters from Table 2. At the end of the calculation the standard deviations of the filter characteristics were calculated. The deviations of the filter characteristics were 0.025 dB for the insertion loss at the pass band frequency, and 3 dB for the rejection at the stop band frequency. Figure 9 presents the transfer function of the filter and the error bars at the pass band and stop band.

3. Conclusions

Using the techniques of digital filter synthesis, it is possible to design filters with very good specifications. Although the theory does not address many practical issues, there are many analysis techniques that can fill the gap to provide the necessary constraints. In the assessment of a real device, the synthesis technique alone will probably not be sufficient. This is because most synthesis techniques will follow some (in the end, arbitrary) rule to simplify the solution space. In the case of the lattice filter, this rule was that the delay in the lattice stages should be the same for each stage. This rule permitted the Z transform formulation and lead to a simplified solution space in which it is possible to construct an optimum design. In the real device, due to errors in fabrication, there is likely to be some deviation in delay from one stage to the next. Assessing the error introduced by this deviation is not possible from within the formulation that employs the Z transform, since the formulation precludes this variation *a priori*. Nevertheless, software-enabled numerical analysis is practical and can answer the questions not addressed by the synthesis technique.

We have designed a lattice filter for an application of isolating an ITU channel from its neighbour and next nearest neighbours. The pass band insertion loss is limited by 0.5 dB, and the stop band rejection is greater than 31 dB. We calculated the error from expected variations in processing (waveguide width). We conclude the effects from this error should be small, only 0.025 dB in the passband and 3 dB in the stop band.

References

- [1] Kaname Jinguji and Masao Kawachi, "Synthesis of Coherent Two-Port Lattice-Form Optical Delay-Line Circuit", *Journal of Lightwave Technology*, **13**(1), p75-82 (1995)
- [2] Christi K. Madsen and Jian H. Zhao, *Optical Filter Design and Analysis, A Signal Processing Approach*, (John Wiley & Sons, New York, 1999)
- [3] Francois Ladouceur and John D. Love, *Silica-based Buried Channel Waveguides and Devices*, (Chapman and Hall, London, 1996)
- [4] Michal Bordovsky, Peter Catrysse, Steven Dods, Marcio Freitas, Jackson Klein, Libor Kotacka, Velko Tzolov, Ivan M. Uzunov, Jiazong Zhang, "Waveguide design, modeling, and optimization: from photonic nanodevices to integrated photonic circuits", *Proc. SPIE Vol. 5355*, p. 65-80, *Integrated Optics: Devices, Materials, and Technologies VIII*; Yakov Sidorin, Ari Tervonen; Eds., (May 2004)
- [5] International Telecommunication Union, G.692 Recommendation on Optical Interfaces for Multichannel Systems with Optical Amplifiers. See also Guide To WDM Technology and Testing, page 15. (EXFO Electro-Optical Engineering Inc. Quebec City, Canada, 2000)
- [6] Christopher J. Kaalund and Gang-Ding Peng, "Pole-Zero Diagram Approach to the Design of Ring Resonator-Based Filters for Photonic Applications", *Journal of Lightwave Technology*, **22**(6), p1548-1559 (2004)
- [7] John G. Proakis and Dimitris G. Manolakis, *Digital Signal Processing, Principles, Algorithms, and Applications*, (Prentice Hall, New Jersey, 1996) Discussion on page 643 to 647.
- [8] Matlab Version 6, a product of The Math Works Inc. (3 Apple Hill Drive, Natick, MA, USA)
- [9] OptiSystem and OptiBPM, products of Optiwave Systems, (7 Capella Ct., Ottawa, K2E 8A7, Canada)
- [10] M. Heiblum and J.H. Harris, "Analysis of Curved Optical Waveguides by Conformal Mapping", *IEEE J. Quant. Electron.* **11**, (1975): 75-83.
- [11] S.J. Garth, "Modes on a Bent Optical Waveguide", *IEEE Proc. J.* **134**, p 221- 229, (1987)
- [12] P.L. Fan, M.L. Wu, and C.T. Lee, "Analysis of Abrupt Bent Waveguides by the Beam Propagation Method and the Conformal Mapping Method", *J. Light. Technol.* **15**, p 1026-1031, (1997)